Biochimica et Biophysica Acta 1858 (2016) 1499–1506

Contents lists available at ScienceDirect

Biochimica et Biophysica Acta

journal homepage: www.elsevier.com/locate/bbamem

# Precise quantification of cellular uptake of cell-penetrating peptides using fluorescence-activated cell sorting and fluorescence correlation spectroscopy

Rachid Rezgui [a], Katy Blumer [b], Gilbert Yeoh-Tan [c], Adam J. Trexler [d], Mazin Magzoub [a,*]

[a] Biology Program, New York University Abu Dhabi, Abu Dhabi, United Arab Emirates
[b] Physics Program, New York University Abu Dhabi, Abu Dhabi, United Arab Emirates
[c] Center for Genomics and Systems Biology (CGSB), New York University Abu Dhabi, Abu Dhabi, United Arab Emirates
[d] Laboratory of Molecular Biophysics, National Heart Lung and Blood Institute, National Institutes of Health, Bethesda, MD, USA

ARTICLE INFO

*Article history:*
Received 7 January 2016
Received in revised form 2 March 2016
Accepted 23 March 2016
Available online 29 March 2016

*Keywords:*
Drug delivery
Cellular uptake
Internalization pathways
Intracellular distribution
Intracellular degradation
Toxicity threshold

ABSTRACT

Cell-penetrating peptides (CPPs) have emerged as a potentially powerful tool for drug delivery due to their ability to efficiently transport a whole host of biologically active cargoes into cells. Although concerted efforts have shed some light on the cellular internalization pathways of CPPs, quantification of CPP uptake has proved problematic. Here we describe an experimental approach that combines two powerful biophysical techniques, fluorescence-activated cell sorting (FACS) and fluorescence correlation spectroscopy (FCS), to directly, accurately and precisely measure the cellular uptake of fluorescently-labeled molecules. This rapid and technically simple approach is highly versatile and can readily be applied to characterize all major CPP properties that normally require multiple assays, including amount taken up by cells (in moles/cell), uptake efficiency, internalization pathways, intracellular distribution, intracellular degradation and toxicity threshold. The FACS–FCS approach provides a means for quantifying any intracellular biochemical entity, whether expressed in the cell or introduced exogenously and transported across the plasma membrane.



## 1. Introduction

Since the discovery of the first cell-penetrating peptides (CPPs) – the TAT peptide (derived from the HIV-1 transcription-activating protein) [1,2] and penetratin (pAntp, from the Antennapedia homeodomain, a *Drosophila* transcription factor) [3] – over two decades ago, CPPs have been used extensively to mediate the cellular delivery of coupled cargoes with high efficiency, both *in vitro* and *in vivo* [4,5]. The wide range of cargoes delivered by CPPs include proteins, peptides, antisense oligonucleotides, small interfering RNAs (siRNAs), λ phages, liposomes, quantum dots, and even 40 nm magnetic iron oxide nanoparticles [4]. Consequently, CPPs have emerged as a potentially powerful tool for drug delivery.

Effective utilization of CPPs for drug delivery requires understanding their cellular internalization mechanisms as well as quantifying their uptake. Although concerted efforts have shed light on the cellular internalization pathways of CPPs [6–8], quantification of CPP uptake has so far proved problematic. The most common approaches for quantifying CPP uptake involve measuring cell-associated fluorescence intensity of cells treated with a fluorescently-labeled CPP and comparing it to the signal from cells treated with a reference peptide or molecule. This is often done with a fluorescence plate reader, flow cytometry, or confocal microscopy [9–12]. Although these methods are straightforward and relatively fast, they compare relative fluorescence intensities and therefore only qualitatively measure uptake.

Another approach involves quantifying the uptake indirectly through a readout generated by a delivered cargo, for instance fluorescent protein expression [13]. A more direct method for measuring cellular internalization of CPPs employs high performance liquid chromatography (HPLC), where a concentration gradient of organic solvent separates elements with different hydrophobic properties to quantify the amount of peptide in cell lysates [14]. Matrix-assisted laser desorption/ionization-time of flight mass spectrometry (MALDI-TOF MS) has also been used to measure peptide concentrations directly by suspending the sample in a matrix that is then vaporized and ionized by a laser, with the particles distinguished by the time of flight through an electric field [15].

However, none of the methods currently available can distinguish healthy cells from unhealthy or dead ones, and so cannot account for peptide cytotoxicity when measuring per-cell concentrations. Even small numbers of dead cells can confound uptake measurements, as cell membranes become porous after death but often stay intact enough

* Corresponding author at: Biology Program, New York University Abu Dhabi, PO Box 129188, Saadiyat Island Campus, Abu Dhabi, United Arab Emirates.
*E-mail address:* mazin.magzoub@nyu.edu (M. Magzoub).

http://dx.doi.org/10.1016/j.bbamem.2016.03.023

to retain peptide which has diffused across the membrane and accumulated intracellularly.

The experimental approach reported here combines two powerful biophysical techniques: fluorescence-activated cell sorting (FACS) and fluorescence correlation spectroscopy (FCS). This rapid and technically straightforward approach is highly versatile and can determine important CPP parameters that normally require multiple assays: intracellular amount, uptake efficiency and internalization pathways.

Notably, the approach has novel capabilities. While most of the current methods for quantifying CPP uptake only measure total cell uptake, the FACS–FCS approach can differentiate CPPs that localize to the cytosol from those trapped in endocytic compartments, and can in turn measure the cytosolic delivery efficiency. And unlike current methods, FACS–FCS distinguishes between healthy and dead cells. Consequently, this approach can be used to accurately quantify the maximum tolerable amounts of CPPs or their cargoes for the cell. Additionally, FACS–FCS can determine the fractions of CPPs that are degraded intracellularly. These are all crucial considerations when utilizing CPPs for drug design and development.

Further, the FACS–FCS approach offers several additional advantages over previously published methods. The combination of FACS and FCS affords the approach greater accuracy and precision, while making it faster and technically simpler than most of the current methods. And since FACS and FCS are widely available at most academic and industrial institutions, this approach is cheaper and more accessible for many researchers. Finally, although we use FACS–FCS here to quantify CPP uptake, it can readily be applied to proteins, peptides, nucleic acids, drugs, or nanoparticles. This generality means that our versatile, rapid and technically straightforward experimental approach should be of broad interest to molecular and cell biologists, biochemists, biophysicists and pharmacologists.

## 2. Materials and methods

### 2.1. Materials

CPPs were synthesized by Selleck Chemicals (Houston, TX) using standard Fmoc methods and purified in house by reverse-phase HPLC (Waters 2535 QGM HPLC). N-terminally biotinylated penetratin (pAntp) was purchased from AnaSpec (Fremont, CA). Alexa Fluor 488 and Alexa Fluor 488-succinimidylester, quantum dot (QD625) streptavidin conjugate, 70 kDa neutral dextran-tetramethylrhodamine, cholera toxin subunit B (recombinant) Alexa Fluor 555 conjugate, transferrin (from human serum) Alexa Fluor 546 conjugate, and wheat germ agglutinin (WGA) Alexa Fluor 594 conjugate (cell membrane marker), were all purchased from Molecular Probes (Carlsbad, CA). 4′,6-diamidino-2-phenylindole (DAPI), propidium iodide (PI), sodium azide, 2-deoxy-D-glucose, and the endocytosis inhibitors – ammonium chloride, chlorpromazine, methyl-β-cyclodextrin, filipin and cytochalasin D – were from Sigma.

### 2.2. Peptide labeling

Amine coupling was used to attach Alexa Fluor 488-succinimidylester to the N-terminus of CPPs as previously described [16]. Briefly, ~0.5 mg of lyophilized peptide was dissolved in 800 μL of 10 mM sodium phosphate, pH 7.2. An approximate 10-fold molar excess of dye (~0.1 mg) was added as powder, and the sample was gently vortexed and incubated on a rotator for 2 h at room temperature. Separation of labeled and un-labeled peptide was done by reverse-phase HPLC, extent of labeling was assessed using mass spectrometry (Agilent 6538 QToF LC/MS), and concentration of labeled protein was determined using absorbance at 494 nm ($\varepsilon = 73000\ M^{-1}\ cm^{-1}$).

N-terminally biotinylated pAntp was labeled with quantum dot (QD625) streptavidin conjugate according to the manufacturer's protocol. Briefly, 1 μL of 1 μM QD625 was mixed with 2 μL of 2 mg/mL biotinylated pAntp in 197 μL PBS (pH 7.4) and incubated for 1 h. Concentration of QD625-labeled pAntp was verified using FCS (see the Fluorescence correlation spectroscopy (FCS) section).

### 2.3. Experimental methods

The FACS–FCS approach involves three major steps: cell preparation and treatment with CPPs, sorting the cells into populations according to CPP uptake, and finally lysing the cells and quantifying the internalized peptide.

#### 2.3.1. Cell preparation and treatment

HeLa cells (ATCC No. CCL-2) were cultured in 5% $CO_2$ in DMEM (Sigma) supplemented with 10% FBS (GE Healthcare Life Sciences, Logan, UT), 4 mM L-glutamine and 1% penicillin/streptomycin (all from Sigma). Once the cells reached ~90% confluence, they were split (using 0.25% trypsin-EDTA, Sigma) and plated at a density of $1 \times 10^6$ cells/well in a 6-well plate (Falcon BD). The seeding density depends on the cell line, and the cells should not exceed 90% confluence, as a high percentage of healthy cells is necessary for obtaining accurate uptake efficiencies. As uptake depends on peptide-to-cell ratio [17], each experiment should have the same number of cells.

After culturing for 48 h, the culture medium was replaced with 2 mL incubation medium (DMEM containing 1 μM fluorescently-labeled CPP), and incubated for 2 h at 37 °C and 5% $CO_2$. To verify the peptide concentration, 1 μL of the incubation medium was diluted to give a final peptide concentration of 10–20 nM, and fluorescence correlation spectroscopy (FCS) was used to measure the number of peptide molecules in the focal volume and hence the concentration (see the Fluorescence correlation spectroscopy (FCS) section).

To study the CPP internalization pathways, the cells were incubated at 4 °C, preincubated with 10 mM sodium azide in the presence of 6 mM 2-deoxy-D-glucose for 1 h to deplete cellular ATP, or pretreated with endocytosis inhibitors: 40 mM ammonium chloride, 10 μM chlorpromazine, 5 mM methyl-β-cyclodextrin, 4 μM filipin or 10 μM cytochalasin D. Note: as the effective concentrations of inhibitors depend on the cell lines and densities used, the inhibitors should be titrated and used at non-toxic concentrations.

Following the treatments, the medium was removed and the cells were washed twice with 2 mL PBS. The cells were dissociated from the wells using 1 mL 0.25% trypsin-EDTA (5 min at 37 °C and 5% $CO_2$) and confocal microscopy was used to verify that all extracellular and membrane-bound peptide was removed during the trypsin treatment (Supplementary Fig. S1). Thereafter, 4 mL cell culture medium was added to inactivate the trypsin, the cells were centrifuged at 100 × *g* for 5 min at 4 °C, and the supernatant was removed. Finally, the cell pellet was resuspended in 2 mL of fresh phenol red-free DMEM, and the total number of cells in the pellet was determined using an automated cell counter (BIO-RAD TC10).

#### 2.3.2. Fluorescence-activated cell sorting (FACS)

FACS [18] was used to rapidly sort the CPP-treated cell sample with a high degree of accuracy and reproducibility. In FACS a cell suspension is entrained in a narrow, rapidly flowing stream of droplets, each containing a single cell. The droplets are electrostatically sorted, one by one, based on a number of attributes, including fluorescence signal, cell size and granularity. The fluorescence signal guarantees that only cells that have taken up peptide are considered, and also provides a very rough measure of uptake that can later be used to corroborate results. Cell size and granularity ensure that only healthy cells are collected, thereby removing the confounding effects of dead or unhealthy cells. Consequently, this approach also allows the experimenter to measure peptide toxicity. Using FACS has the added benefit of providing an accurate cell count to later calculate the exact amount of peptide taken up per cell.

FACS (BD FACSAria III, BD Biosciences) was used to sort 500,000 healthy cells per experiment. The cells were sorted according

fluorescence signal vs forward/side scatter (FSC/SSC) analysis. The population with a strong fluorescence signal was isolated, ensuring that it has a narrow distribution on the FSC/SSC plot to eliminate dead cells and debris (Supplementary Fig. S2). To determine the toxicity threshold, populations of cells that have taken up the peptide were stained with DAPI/PI (1 μM for 10 min) and further sorted into live/dead subpopulations, using the DAPI (live cells) and PI (dead cells) signals, and the fractions of the live/dead subpopulations relative to the total number of cells in that population was determined.

Following sorting, the volumes of the different populations were measured and the populations were centrifuged at 100 × *g* for 5 min, 4 °C, to pellet the cells. The supernatant was then removed and the pellet was resuspended in 100 μL lysis buffer (CellLytic™, Sigma) and incubated for 1 h on ice. Finally, the lysate was diluted 10 fold in PBS.

The cytosolic fraction was isolated as previously described [19]. Briefly, following sorting and pelleting of cells that have taken up the peptide, the pellet was resuspended in 500 μL ice cold isotonic buffer (250 mM sucrose, 50 mM Tris–HCl pH 7.4, 5 mM $MgCl_2$, protease and phosphatase inhibitor cocktails; all from Sigma) in a glass centrifuge tube. Cells were homogenized for 30 s on ice using a tight-fitting Teflon pestle attached to a Potter S homogenizer (Sartorius, Göttingen, Germany) set to 150 rpm, and lysis was verified by phase contrast light microscopy. The homogenate was then sedimented by centrifugation on a table-top ultracentrifuge at 100,000 × *g* for 30 min at 4 °C. Finally, the supernatant (cytosolic fraction) was collected.

*2.3.3. Fluorescence correlation spectroscopy (FCS)*

FCS was used to measure the exact amount of CPPs taken up by the cells in the lysate. FCS is a quantitative technique with single molecule sensitivity that measures fluorescence intensity fluctuations when a small number of fluorescently labeled molecules diffuse through a small (~1.6 femtoliter) focal volume (Supplementary Fig. S3A and B). Autocorrelation (self-similarity) of the signal accurately determines the diffusion dynamics and the number of fluorescently labeled molecules in the sampling volume (Supplementary Fig. S3C). Thus FCS can be used to directly measure intracellular fluorophore concentrations in the nanomolar range. Measurements of diffusion also directly report on changes in the size of the molecule of interest due to, for instance, degradation, aggregation or binding. Moreover, FCS possesses the advantage of being fast and easy to calibrate, which makes it ideal for quantifying cellular uptake.

FCS measurements were done on a home-built FCS system equipped with the appropriate filter sets and a high numerical aperture (NA) objective for FCS (e.g. 60× or 100×, water or oil immersion). The laser power was adjusted to 20–100 μW. 50 μL of a 5 nM solution of Alexa 488 dye was placed on a microscope slide and the optimal objective position for FCS was located (the detector was used to find the upper slide surface, i.e. the plane with highest signal, and the focal point was moved 10 μm above the upper slide surface). Data points were acquired for 30 s with an avalanche photodiode detector (APD) and the autocorrelation curve calculated using a correlator (ALV-7004/USB). The autocorrelation curve was then fit to the following function to determine focal volume radii $\omega_{x,y,z}$, given the concentration and the diffusion coefficient, *D*, of the dye (*D* depends on the dye and the experimental conditions, such as the solvent viscosity and the temperature; for Alexa 488 in water at 25 °C, $D = 435\ \mu m^2/s$) [20]:

$$G(\tau) = G(0)\frac{1}{\left(1+\left(\frac{\tau}{\tau_D}\right)\right)\cdot\sqrt{\left(1+\left(\frac{\omega_{xy}}{\omega_z}\right)^2\cdot\left(\frac{\tau}{\tau_D}\right)\right)}} \quad (1)$$

where $G(0)$ is the inverse of the number of molecules, *N*, present in the focal volume, and $\tau_D$ is the average diffusion time a molecule takes to transit the focal volume. The relation between the diffusion coefficient, *D*, and $\tau_D$ is given by:

$$D = \frac{\omega_{xy}^2}{4\tau_D} \quad (2)$$

The focal volume was calibrated over a wide range of concentrations (ideally, this should be done at the start of each new experiment). Solutions of 2.5, 5, 10, 25, 50 and 100 nM Alexa 488 were prepared in buffer, and for each solution 50 μL was placed on a slide keeping the droplet radius as small as possible. The number of molecules in the focal volume, *N*, was determined using Eq. (1) and plotted as a function of the known dye concentration and a linear fit performed (Supplementary Fig. S3D). The focal volume was then determined by dividing the slope of the linear fit by a correction factor. This correction factor is derived from converting the concentration (in nM) to number of molecules per femtoliter (using: number of molecules per volume = molar concentration × Avogadro's number) and corresponds to 1 nM = 0.6 molecules per femtoliter.

To measure the CPP concentration in the cell lysates, each sample was centrifuged at 300 × *g* for 10 s, 25 °C, immediately prior to measurement, and 50 μL was pipetted onto a microscope slide. The number of molecules in the volume, *N*, and the diffusion coefficient, *D*, were determined using Eq. (1).

For samples containing peptide particles of different sizes (and therefore different diffusion coefficients), e.g. as a result of intracellular peptide degradation, the autocorrelation curve was instead fit to the following multiple-component function [21]:

$$G(\tau) = G(0)\sum_{i=1}^{n}\frac{f_i}{\left(1+\left(\frac{\tau}{\tau_{D,i}}\right)\right)\cdot\sqrt{\left(1+\left(\frac{\omega_{xy}}{\omega_z}\right)^2\cdot\left(\frac{\tau}{\tau_{D,i}}\right)\right)}} \quad (3)$$

to determine the number of particles, *N*, the diffusion time, $\tau_{D,i}$, and the fractional population, $f_i$, of *n* different diffusion particles with $\sum f_i = 1$, using the focal volume determined with the Alexa 488 dye and Eq. (1).

*N* was divided by the focal volume determined previously to obtain the peptide concentration. Finally, the number of sorted cells and volume of the lysate solution was used to determine the amount of internalized CPP per cell, while the initial peptide concentration and cell number were used to determine the uptake efficiency.

## 3. Results and discussion

The rapid and technically straightforward experimental approach reported here is highly versatile and can readily be used to determine all the major properties of CPPs that are important for their drug delivery applications. These properties include amount taken up by cells (in moles/cell), uptake efficiency, mechanism of cellular internalization, intracellular distribution, intracellular degradation and cytotoxicity threshold.

### 3.1. Quantification of CPP uptake

The concentration calibration curve performed in buffer (Supplementary Fig. S3D) was repeated in cell lysates to determine whether binding to cellular components could distort the concentration measurements. Increasing concentrations of Alexa 488 were diluted in HeLa cell lysates and the number of molecules in the focal volume, *N*, was determined using Eq. (1) and plotted as a function of known dye concentration (Fig. 1A). The linear relation between *N* and known concentration clearly shows that no significant binding takes place between the dye molecules and cellular components in the lysates.

We applied FACS–FCS to measure the cellular internalization of penetratin (pAntp), one of the most widely studied CPPs [4], into HeLa

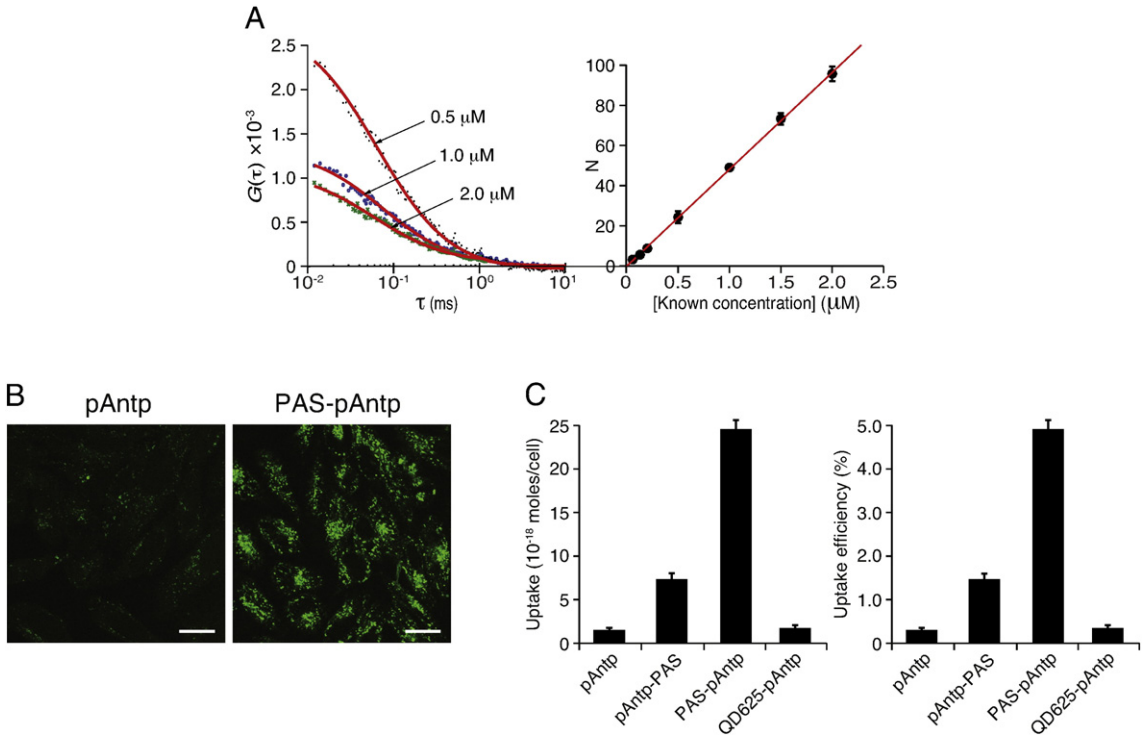


**Fig. 1.** Quantification of cellular uptake of CPPs. (A) Calibration curve in HeLa cell lysates. Increasing concentrations of Alexa 488 were diluted in HeLa cell lysates and the number of molecules in the focal volume, *N*, was determined from the autocorrelation curves (*left*) using Eq. (1). *N* was then plotted as a function of the known dye concentration (*right*). (B, C) Comparison of cellular uptake of related CPPs. $1 \times 10^6$ HeLa cells were treated with 1 μM Alexa 488-labeled CPPs for 2 h. (B) Confocal images of cellular uptake of pAntp (*left panel*) and PAS–pAntp (*right panel*). Scale bar = 10 μm. (C) Following peptide incubation, cells were washed and trypsinized and confocal microscopy was used to confirm removal of all membrane-bound peptide. The cells were sorted using fluorescence-activated cell sorting (FACS) according to intracellular fluorescence signal, with the forward vs side scatter (FSC vs SSC) analysis used to discard dead cells and debris. Finally, the CPP-positive cells were lysed and FCS was used to measure the precise number of internalized CPPs. The cell uptake can be presented as either (*left*) the absolute number of internalized CPPs (expressed in moles/cell) or (*right*) the uptake efficiency of the CPPs relative to the initial peptide concentration exposed to the cells. Error bars represent standard error across three or more independent trials.

cells. The peptide was N-terminally labelled with Alexa Fluor 488-succinimidylester [16] or quantum dots (QD625). We also quantified cellular uptake of pAntp sequences that were covalently coupled either N- or C-terminally to a penetration accelerating sequence (PAS) [23], PAS–pAntp or pAntp–PAS, respectively, and labeled with Alexa Fluor 488 (Table 1). Coupling of the short PAS segment (FFLIPKG) to CPPs has been shown to enhance their intracellular delivery and cytosolic release [23].

We found that the uptake of Alexa 488 labeled pAntp was $1.7 \pm 0.3 \times 10^{-18}$ moles/cell (Fig. 1C). Similar uptake was observed for the QD625 labeled peptide, indicating that the amount of pAntp taken up by the cells is not affected by the nature of fluorophore used to label the peptide. Covalently coupling PAS to the C-terminus of pAntp (pAntp–PAS) enhanced uptake 4-fold compared to pAntp (Fig. 1C), whereas coupling PAS N-terminal to pAntp (PAS–pAntp) lead to substantial enhancement in cellular internalization (Fig. 1B), with the uptake approximately 15-fold of pAntp (Fig. 1C).

Similar effects of PAS on the cellular internalization of another CPP, octaarginine, were reported in a previous study [23]. However, that study used FACS and confocal microscopy to provide relative measures of intracellular fluorescence intensities, whereas we use a more sensitive technique, FCS, to directly measure uptake. Thus, this rapid and straightforward approach can directly measure the number of moles of CPP per cell, and in turn determine the uptake efficiency, precisely and accurately down to the low nanomolar range, which is the expected physiological range for CPP uptake.

**Table 1**
CPPs characterized using FACS–FCS.

| Peptide | Sequence | References |
|---|---|---|
| pAntp | A488-RQIKIWFQNRRMKWKK | [5] |
| pAntp–PAS | A488-RQIKIWFQNRRMKWKKGKPILFF | – |
| PAS–pAntp | A488-FFLIPKGRQIKIWFQNRRMKWKK | – |
| QD625-pAntp | QD625-RQIKIWFQNRRMKWKK | [22] |

### 3.2. Cellular uptake mechanisms of CPPs

The FACS–FCS experimental approach can readily delineate the contribution of active processes such as endocytosis and passive, energy-independent mechanisms (e.g. pore-formation) to the cellular internalization of CPPs (Fig. 2). Both active and passive mechanisms of uptake have been reported for CPPs [24–26]. Further, in the case of an active uptake mechanism FACS–FCS can be used, in conjunction with endocytosis inhibitors, to determine the contribution of different endocytic routes to the uptake.

Lowering the temperature to 4 °C, where all energy-dependent uptake processes are inhibited, resulted in near complete inhibition of pAntp uptake into HeLa cells (Fig. 2A and Supplementary Fig. S4B). Likewise, depleting the cellular ATP pool by preincubation of the cells with sodium azide and deoxyglucose [27,28] led to a substantial reduction in cellular internalization of pAntp (Supplementary Fig. S5A). Taken together, these results indicate that the cellular internalization of the peptide is largely through an active, energy-dependent uptake mechanism. This is supported by the observation that treatment with ammonium chloride, a lysosomotropic agent that inhibits the acidification of internal vesicles such as late endosomes and lysosomes, considerably reduced the amount of internalized pAntp (Fig. 2A and Supplementary Fig. S4C).

In order to determine whether this energy-dependent uptake mechanism involves a specific endocytic pathway, the cells were pretreated with endocytosis inhibitors (Fig. 2A). As a control, we verified the

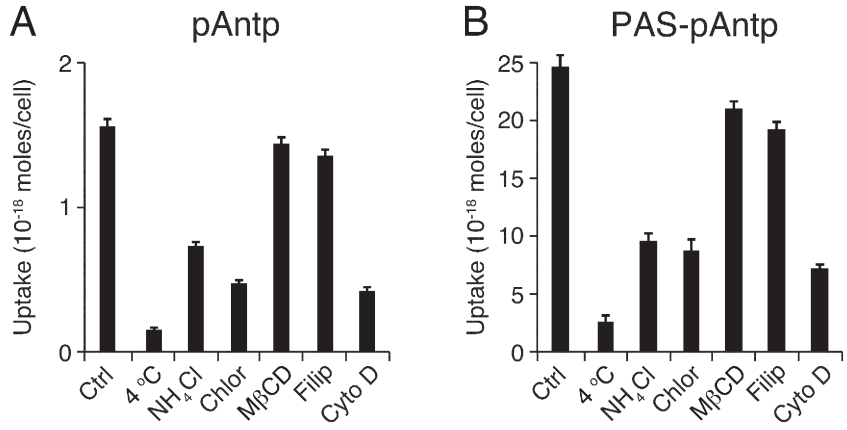


**Fig. 2.** Determination of CPP cellular uptake mechanisms. $1 \times 10^6$ HeLa cells were incubated at 4 °C to inhibit all energy-dependent processes, or were pre-treated with specific endocytosis inhibitors for 1 h. The inhibitors used were: 40 mM ammonium chloride (acidification of endocytic vesicles), 10 μM chlorpromazine (chlor; clathrin-dependent endocytosis), 5 mM methyl-β-cyclodextrin (lipid raft-mediated endocytosis), 4 μM filipin (caveolae-dependent endocytosis), or 10 μM cytochalasin D (cyto D; macropinocytosis). Cells were then treated for 2 h with 1 μM (A) pAntp or (B) PAS–pAntp labeled with Alexa 488. Following peptide incubation, cells were washed, trypsinized and sorted using FACS. Finally, peptide uptake was quantified by FCS (S.E., n = 3).

efficacy of the endocytic inhibitors, at the doses used, by determining their effect on the cellular uptake of established endocytosis markers: transferrin-Alexa 546 (clathrin-mediated endocytosis), cholera toxin B subunit-Alexa 555 (caveolae-dependent endocytosis), and 70 kDa neutral dextran-tetramethylrhodamine (macropinocytosis) [8,29,30]. The results are summarized in Supplementary Fig. S6A. Additionally, we confirmed that all the inhibitors did not affect cell viability at the concentrations used (Supplementary Fig. S6B).

First, we inhibited clathrin-mediated endocytosis, the best characterized endocytosis pathway, using chlorpromazine, which inhibits clathrin-coated pit formation [31]. Treatment with chlorpromazine resulted in a marked reduction in the amount of internalized pAntp. Next, the cells were treated with methyl-β-cyclodextrin to remove cholesterol from the plasma membrane, which disrupts several lipid raft-mediated endocytic pathways, including caveolae-dependent endocytosis and macropinocytosis [32–34]. Disruption of lipid rafts by methyl-β-cyclodextrin had a negligible effect on the cellular uptake of pAntp, indicating that peptide internalization is lipid raft-independent. This was confirmed by treating cells with filipin, an inhibitor of lipid raft-mediated caveolae endocytosis [32,35], which again had little effect on the uptake of the peptide. On the other hand, treatment with cytochalasin D, a specific inhibitor of F-actin elongation involved in macropinocytosis [36], substantially reduced the amount of internalized pAntp (Fig. 2A and Supplementary Fig. S4D). Similar effects were observed for the pAntp variant that exhibited the highest uptake efficiency, PAS–pAntp (Fig. 2B and Supplementary Fig. S5B). Taken together these results show that cellular uptake of pAntp and its variants occurs primarily through clathrin-dependent endocytosis and macropinocytosis. These results are in agreement with previously published studies, with internalization by both clathrin-dependent endocytosis and macropinocytosis reported for pAntp [5], and underline the robustness of the approach.

It should be noted that cellular uptake by various mechanisms has been reported for CPPs. The particular CPP cellular internalization mechanism appears to be highly dependent on peptide concentration. At the low peptide concentrations used in this study (i.e. 1–2 μM), endocytosis was shown to be the primary route of entry for pAntp and other CPPs; at higher concentrations (generally > 10 μM), cellular uptake was observed to occur through direct translocation via energy-independent pathways [37,38]. Cellular uptake pathways of CPPs are also likely to be influenced by other experimental parameters, such as cell line, incubation time, presence or absence of serum, as well as the characteristics of a coupled cargo (including a fluorophore used to label the peptide) and the coupling strategy [7,8,39,40]. We are currently investigating the influence of all of these parameters on the cellular uptake pathways of the CPPs used in this study.

### 3.3. Intracellular distribution of CPPs

An important criterion for assessing the drug delivery potential of CPPs is the efficiency with which they escape from endosomes and lysosomes and localize to the cytosol. However, most of the current methods for quantifying CPP uptake only measure total cell uptake. In contrast, the approach reported here can readily differentiate molecules in the cytosol from those trapped in endocytic compartments, and can in turn measure the cytosolic delivery efficiency.

To determine the intracellular distributions of the CPPs in HeLa cells, the cytosolic fractions were isolated from cells that had taken up the peptides by homogenization of the cells followed by ultracentrifugation. FCS was then used to quantify the amount of CPPs that localize to the cytosol (Fig. 3A). We found that virtually all of the intracellular pAntp is trapped in endocytic compartments, with only $3.3 \pm 0.8 \times 10^{-20}$ moles/cell (or ~2% of internalized pAntp) reaching the cytosol. Interestingly, in a recent study using FCS measurements in live cells the cytosolic delivery efficiency of another widely studied CPP, the HIV-1 TAT-derived peptide, was determined to be 2% of the total amount of peptide taken up the cells [19]. On the other hand, the PAS coupled peptides exhibited a much higher cytosolic delivery efficiency, with $1.0 \pm 0.2 \times 10^{-18}$ and $7.4 \pm 0.9 \times 10^{-18}$ moles/cell of pAntp–PAS and PAS–pAntp, respectively, trafficking to the cytosol from the endocytic pathway (Fig. 3A). This corresponds to ~ 15% and 30% of internalized pAntp–PAS and PAS–pAntp, respectively, reaching the cytosol.

Membrane active peptides, such as CPPs, often perturb and weaken lipid bilayers [4]. Thus, a potential source of error is that the homogenization step would result in lysis of the weakened endosomal membranes, leading to release of entrapped CPPs and overestimation of their cytosolic delivery. As a control, HeLa cells were treated with 70 kDa neutral dextran-tetramethylrhodamine, alone or with non-covalently attached CPPs, and FCS was used to quantify the amount of dextran in the cytosolic fraction. In all cases, leakage of the 70 kDa dextran from endosomes to the cytosol was negligible (Supplementary Fig. S7A), demonstrating that the homogenization protocol used here does not result in lysis of CPP-entrapping endosomes.

Another concern is that following escape from endocytic compartments, CPPs bind to intracellular membranes and are then removed by the ultracentrifugation step leading to an underestimation of the cytosolic delivery efficiency. Therefore, as a control, Alexa 488-labeled CPPs were added to HeLa cell homogenates, and FCS was used to

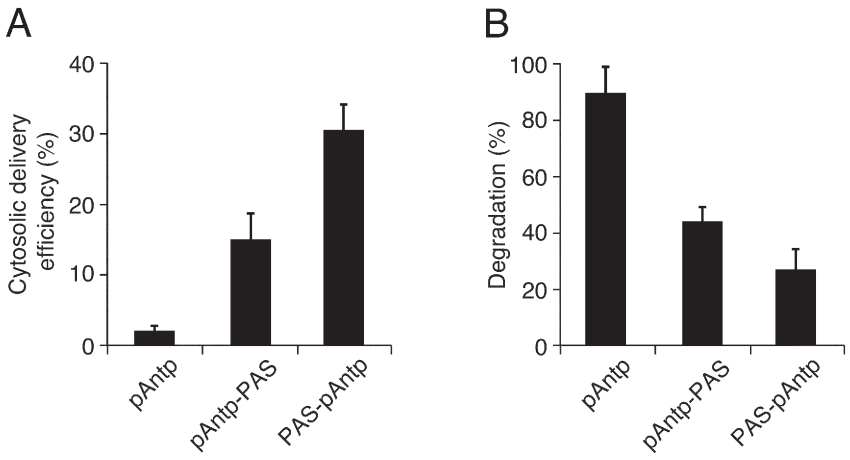


**Fig. 3.** Intracellular distribution and degradation of CPPs. $1 \times 10^6$ HeLa cells were treated with 1 μM Alexa 488-labeled CPPs for 2 h. Following peptide incubation, cells were washed, trypsinized and sorted by FACS according to intracellular fluorescence signal. FCS was then used to measure (A) the amount of CPPs in the cytosolic fraction (isolated by homogenization of the cells followed by ultracentrifugation), or (B) the amount of CPPs that is degraded intracellularly, both relative to the amount of peptide taken up by the cells (S.E., n = 3).

measure the amount of CPP in the cytosolic fractions isolated by ultracentrifugation. For each of the CPPs, all of the peptide added to the homogenate was recovered in the cytosolic fraction (Supplementary Fig. S7B), indicating that loss of cytosolic CPPs due to binding to intracellular membranes is negligible.

Thus coupling of pAntp to PAS not only substantially enhances cellular uptake by endocytosis (Figs. 1 and 2), but also dramatically increases endosomal escape and cytosolic localization of the peptide (Fig. 3A). Similar effects of PAS on the localization patterns of the octaarginine CPP in HeLa cells were observed by confocal microscopy [23].

### 3.4. Intracellular degradation of CPPs

Another important consideration is the metabolic stability of CPPs. On the one hand, CPPs need to remain intact long enough to efficiently deliver their cargoes to intracellular target sites. On the other hand, degradation of CPPs ensures release of the chemically conjugated cargoes, minimizes the risk of unforeseen effects of the peptide, and eliminates the possibility of the peptide-cargo conjugate 'leaking back' to the extracellular environment. Consequently, a balance needs to be struck between avoiding premature cleavage of the CPP and freeing the cargo and clearing the peptide once the cargo has been delivered.

To assess the suitability of FACS–FCS for quantifying CPP degradation, mixtures of Alexa 488-labeled PAS–pAntp and free Alexa 488 dye, at different molar ratios, were added to HeLa cell lysates. The FCS autocorrelation curves were then fit to a multiple-component function describing the diffusion of particles with different sizes (Eq. (3)) to determine the fractional populations of CPP and dye in the lysate. The results are summarized in Supplementary Fig. S8, showing excellent agreement between the experimentally measured CPP and dye fractional populations in the lysates and the CPP and dye molar ratios in the mixtures added to the lysates.

Following CPP incubation, the cells were washed, trypsinized and sorted by FACS according to intracellular fluorescence signal. The CPP-positive cells were then lysed, and the autocorrelation data from the cell lysates was fit to Eq. (3) to determine the fractions of CPPs that are degraded intracellularly (Fig. 3B). The results show that nearly 90% of intracellular pAntp is degraded. Similar extensive degradation of pAntp following cellular uptake has been reported by others [41,42]. However, coupling of pAntp to PAS substantially reduces the intracellular degradation, with over 70% of internalized PAS–pAntp remaining intact. Interestingly, the decrease in degradation correlates with increased cytosolic delivery efficiency (Fig. 3A), indicating that escape from the endosomal pathway, following cellular uptake, protects the PAS-coupled CPPs from degradation. These results identify endocytic compartments as the major site of degradation, which is supported by previous studies where lysosomal protease inhibitors were found to inhibit the intracellular degradation of pAntp [43]. Our results also suggest that once the PAS-coupled CPPs traffic to the cytosol, they rapidly localize to proteolytically privileged sites where they are shielded from cytoplasmic proteases [42].

### 3.5. CPP toxicity threshold

Unlike current methods for measuring CPP uptake, the FACS–FCS approach can also be used to study the cytotoxic effects of CPPs or their cargoes and to accurately determine the maximum tolerable amounts for the cell.

Following incubation of HeLa cells with the CPP that exhibited the highest uptake efficiency, PAS–pAntp, cells were sorted into populations according to peptide uptake. These populations were further sorted into live/dead subpopulations using DAPI/PI staining. Cell viability/toxicity was then determined by quantifying the fractions of the live/dead subpopulations relative to the total number of cells in that population. Finally, cell viability was plotted as a function of the amount of PAS–pAntp taken up by the cells in the total population (Fig. 4).

Plasma membrane disruptions often spontaneously and rapidly reseal [44]. Thus, a potential concern is that transient membrane disruption due to the CPPs would be undetected by our cell viability/toxicity protocol. To determine whether the Alexa 488-labeled PAS–pAntp temporarily disrupts the plasma membrane during the course of peptide exposure, we compared the cell viability measured using DAPI/PI staining after sorting by FACS (i.e. our original protocol) vs staining during peptide exposure. As summarized in Supplementary Fig. S9, DAPI/PI staining during peptide exposure rather than after sorting did not alter the measured cell viabilities, indicating that exposure to Alexa 488-PAS–pAntp does not transiently disrupt the cell membrane. The FACS–FCS experimental approach therefore enables determination of the toxicity threshold of CPPs or their cargoes, which is a key parameter in assessing suitability for drug delivery.

The presence of cargo is likely to influence not only the mechanism of internalization of CPPs, but also their cytotoxic effects. Cargo characteristics such as size, charge and conjugation methodology have been all been shown to affect CPP cytotoxicity [7,45,46]. Given that fluorescent dyes are often highly hydrophobic molecules that interact with cellular membranes, the presence of these fluorophore cargoes would be expected to enhance the cytotoxic effects of CPPs relative to the peptide alone. We are currently conducting follow-up studies to fully

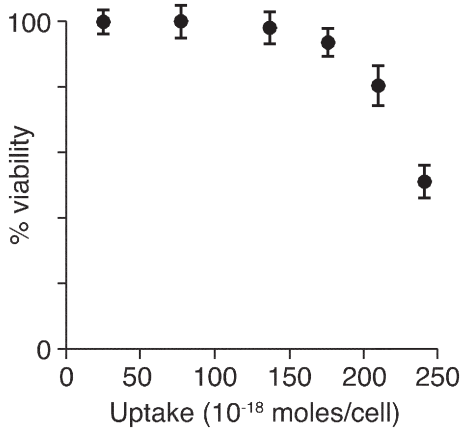


**Fig. 4.** Cell viability as a function of amount of internalized CPP. $1 \times 10^6$ HeLa cells were treated with 1 μM Alexa 488-labeled PAS–pAntp for 2–4 h. Following peptide incubation, cells were washed, trypsinized and sorted using FACS according to intracellular fluorescence signal. Populations of cells that took up peptide were then stained with DAPI/PI (1 μM for 10 min) and sorted further into live/dead subpopulations, using the DAPI (live cells) and PI (dead cells) signals. Finally, the fractions of the live/dead subpopulations were determined relative to the total number of cells in that population, and FCS was used to measure the precise amount of internalized CPP in the total population (S.E., n = 3).

characterize the effect of different cargoes (including fluorophores), as well as coupling strategies, on the cytotoxicity of CPPs.

## 4. Conclusions

The rapid and technically straightforward FACS–FCS experimental approach directly, accurately and precisely measures the number of moles of CPPs per cell down to the low nanomolar range, which is the expected physiological range for CPP uptake. From this the CPP uptake efficiency can be determined. FACS–FCS can also delineate the contribution of active (e.g. endocytosis) and passive (energy-independent, e.g. pore-formation) processes to the cellular internalization mechanism. In the case of an active uptake mechanism, the approach can be used in conjunction with endocytosis inhibitors to determine the contribution of different endocytic routes to the uptake. FACS–FCS readily differentiates CPPs that localize to the cytosol from those trapped in endocytic compartments, and in turn measures the cytosolic delivery efficiency of the peptides. The approach can also be applied to measure the cytotoxicity threshold of CPPs through live/dead cell counts at the FACS step. Finally, the diffusion measurements by FCS report on the fraction of peptide that is degraded or aggregated intracellularly, or bound to an intracellular structure. Thus, FACS–FCS can be used to assess all the major properties of CPPs that are important for their drug delivery applications. Although we use the experimental approach here to quantify intracellular CPPs, it can readily be applied to all biomolecules (proteins, peptides, nucleic acids, drugs or nanoparticles) that are either expressed in the cell or introduced exogenously and transported across the plasma membrane.

Supplementary data to this article can be found online at http://dx.doi.org/10.1016/j.bbamem.2016.03.023.

## Author contributions

M.M. and A.J.T. conceived the research. M.M. and R.R. designed the experiments, and R.R. and K.B. performed the experiments. G.Y.-T. provided technical help. M.M., R.R. and K.B. analyzed the data and wrote the manuscript.

## Competing financial interests

The authors declare that they have no competing financial interests.

## Transparency document

The Transparency document associated with this article can be found, in online version.

## Acknowledgments

The authors thank Justin Blau (NYU), Andrew Miranker (Yale University) and Elizabeth Rhoades (Yale University) for comments on the manuscript. Confocal imaging experiments were carried out using the Core Technology Platform resources at NYU Abu Dhabi. This work was supported by a start-up fund for M.M. from NYU Abu Dhabi. Additional support was provided by NYU Abu Dhabi Institute Grant G1205. A.J.T. received support from the National Institutes of Health (F31 AG038110).

## References

[1] M. Green, P.M. Loewenstein, Autonomous functional domains of chemically synthesized human immunodeficiency virus tat trans-activator protein, Cell 55 (1988) 1179–1188.
[2] A.D. Frankel, C.O. Pabo, Cellular uptake of the tat protein from human immunodeficiency virus, Cell 55 (1988) 1189–1193.
[3] A. Joliot, C. Pernelle, H. Deagostini-Bazin, A. Prochiantz, Antennapedia homeobox peptide regulates neural morphogenesis, Proc. Natl. Acad. Sci. U. S. A. 88 (1991) 1864–1868.
[4] M. Magzoub, A. Gräslund, Cell-penetrating peptides: [corrected] from inception to application, Q. Rev. Biophys. 37 (2004) 147–195.
[5] E. Dupont, A. Prochiantz, A. Joliot, Penetratin story: an overview, in: Ü. Langel (Ed.), Cell-Penetrating Peptides, Humana Press 2011, pp. 21–29.
[6] M. Magzoub, A. Pramanik, A. Gräslund, Modeling the endosomal escape of cell-penetrating peptides: transmembrane pH gradient driven translocation across phospholipid bilayers†, Biochemistry 44 (2005) 14890–14897.
[7] F. Madani, S. Lindberg, Ü. Langel, S. Futaki, A. Gräslund, Mechanisms of cellular uptake of cell-penetrating peptides, J. Biophys. 2011 (2011).
[8] J.S. Wadia, R.V. Stan, S.F. Dowdy, Transducible TAT-HA fusogenic peptide enhances escape of TAT-fusion proteins after lipid raft macropinocytosis, Nat. Med. 10 (2004) 310–315.
[9] A. Florén, I. Mäger, Ü. Langel, Uptake kinetics of cell-penetrating peptides, in: Ü. Langel (Ed.), Cell-Penetrating Peptides, Humana Press 2011, pp. 117–128.
[10] R.H. Mo, J.L. Zaro, W.-C. Shen, Comparison of cationic and amphipathic cell penetrating peptides for siRNA delivery and efficacy, Mol. Pharm. 9 (2012) 299–309.
[11] I. Mäger, E. Eiríksdóttir, K. Langel, S.E.L. Andaloussi, Ü. Langel, Assessing the uptake kinetics and internalization mechanisms of cell-penetrating peptides using a quenched fluorescence assay, Biochim. Biophys. Acta Biomembr. 1798 (2010) 338–343.
[12] G. Drin, S. Cottin, E. Blanc, A.R. Rees, J. Temsamani, Studies on the internalization mechanism of cationic cell-penetrating peptides, J. Biol. Chem. 278 (2003) 31192–31201.
[13] S.E. Andaloussi, P. Guterstam, Ü. Langel, Assessing the delivery efficacy and internalization route of cell-penetrating peptides, Nat. Protoc. 2 (2007) 2043–2047.
[14] T. Holm, H. Johansson, P. Lundberg, M. Pooga, M. Lindgren, Ü. Langel, Studying the uptake of cell-penetrating peptides, Nat. Protoc. 1 (2006) 1001–1005.
[15] F. Burlina, S. Sagan, G. Bolbach, G. Chassaing, Quantification of the cellular uptake of cell-penetrating peptides by MALDI-TOF mass spectrometry, Angew. Chem. Int. Ed. 44 (2005) 4244–4247.
[16] M. Magzoub, A.D. Miranker, Concentration-dependent transitions govern the subcellular localization of islet amyloid polypeptide, FASEB J. 26 (2012) 1228–1238.
[17] M. Hällbrink, J. Oehlke, G. Papsdorf, M. Bienert, Uptake of cell-penetrating peptides is dependent on peptide-to-cell ratio rather than on peptide concentration, Biochim. Biophys. Acta Biomembr. 1667 (2004) 222–228.
[18] W.A. Bonner, H.R. Hulett, R.G. Sweet, L.A. Herzenberg, Fluorescence activated cell sorting, Rev. Sci. Instrum. 43 (1972) 404–409.
[19] J.R. LaRochelle, G.B. Cobb, A. Steinauer, E. Rhoades, A. Schepartz, Fluorescence correlation spectroscopy reveals highly efficient cytosolic delivery of certain penta-arg proteins and stapled peptides, J. Am. Chem. Soc. 137 (2015) 2536–2541.
[20] Z. Petrášek, P. Schwille, Precise measurement of diffusion coefficients using scanning fluorescence correlation spectroscopy, Biophys. J. 94 (2008) 1437–1448.
[21] K. Weisshart, V. Jüngel, S.J. Briddon, The LSM 510 META — ConfoCor 2 system: an integrated imaging and spectroscopic platform for single-molecule detection, Curr. Pharm. Biotechnol. 5 (2004) 135–154.
[22] B.R. Liu, Y.-W. Huang, H.-J. Chiang, H.-J. Lee, Cell-penetrating peptide-functionized quantum dots for intracellular delivery, J. Nanosci. Nanotechnol. 10 (2010) 7897–7905.
[23] K. Takayama, I. Nakase, H. Michiue, T. Takeuchi, K. Tomizawa, H. Matsui, S. Futaki, Enhanced intracellular delivery using arginine-rich peptides by the addition of penetration accelerating sequences (Pas), J. Control. Release 138 (2009) 128–133.
[24] I.D. Alves, C.-Y. Jiao, S. Aubry, B. Aussedat, F. Burlina, G. Chassaing, S. Sagan, Cell biology meets biophysics to unveil the different mechanisms of penetratin internalization in cells, Biochim. Biophys. Acta Biomembr. 1798 (2010) 2231–2239.

[25] H. Hirose, T. Takeuchi, H. Osakada, S. Pujals, S. Katayama, I. Nakase, S. Kobayashi, T. Haraguchi, S. Futaki, Transient focal membrane deformation induced by arginine-rich peptides leads to their direct penetration into cells, Mol. Ther. 20 (2012) 984–993.
[26] M.M. Fretz, N.A. Penning, S. Al-Taei, S. Futaki, T. Takeuchi, I. Nakase, G. Storm, A.T. Jones, Temperature-, concentration- and cholesterol-dependent translocation of L- and D-octa-arginine across the plasma and nuclear membrane of CD34+ leukaemia cells, Biochem. J. 403 (2007) 335–342.
[27] J.P. Richard, K. Melikov, E. Vives, C. Ramos, B. Verbeure, M.J. Gait, L.V. Chernomordik, B. Lebleu, Cell-penetrating peptides a reevaluation of the mechanism of cellular uptake, J. Biol. Chem. 278 (2003) 585–590.
[28] A.P. Manceur, B.D. Driscoll, W. Sun, J. Audet, Selective enhancement of the uptake and bioactivity of a TAT-conjugated peptide inhibitor of glycogen synthase kinase-3, Mol. Ther. 17 (2008) 500–507.
[29] P.A. Orlandi, P.H. Fishman, Filipin-dependent inhibition of cholera toxin: evidence for toxin internalization and activation through caveolae-like domains, J. Cell Biol. 141 (1998) 905–915.
[30] C. Le Roy, J.L. Wrana, Clathrin- and non-clathrin-mediated endocytic regulation of cell signalling, Nat. Rev. Mol. Cell Biol. 6 (2005) 112–126.
[31] L.H. Wang, K.G. Rothberg, R.G. Anderson, Mis-assembly of clathrin lattices on endosomes reveals a regulatory switch for coated pit formation, J. Cell Biol. 123 (1993) 1107–1117.
[32] R.G.W. Anderson, The caveolae membrane system, Annu. Rev. Biochem. 67 (1998) 199–225.
[33] B.J. Nichols, J. Lippincott-Schwartz, Endocytosis without clathrin coats, Trends Cell Biol. 11 (2001) 406–412.
[34] N.Q. Liu, A.S. Lossinsky, W. Popik, X. Li, C. Gujuluva, B. Kriederman, J. Roberts, T. Pushkarsky, M. Bukrinsky, M. Witte, M. Weinand, M. Fiala, Human immunodeficiency virus type 1 enters brain microvascular endothelia by macropinocytosis dependent on lipid rafts and the mitogen-activated protein kinase signaling pathway, J. Virol. 76 (2002) 6689–6700.
[35] J.E. Schnitzer, P. Oh, E. Pinney, J. Allard, Filipin-sensitive caveolae-mediated transport in endothelium: reduced transcytosis, scavenger endocytosis, and capillary permeability of select macromolecules, J. Cell Biol. 127 (1994) 1217–1232.
[36] P. Sampath, T.D. Pollard, Effects of cytochalasin, phalloidin, and pH on the elongation of actin filaments, Biochemistry 30 (1991) 1973–1980.
[37] F. Duchardt, M. Fotin-Mleczek, H. Schwarz, R. Fischer, R. Brock, A comprehensive model for the cellular uptake of cationic cell-penetrating peptides, Traffic 8 (2007) 848–866.
[38] M. Kosuge, T. Takeuchi, I. Nakase, A.T. Jones, S. Futaki, Cellular internalization and distribution of arginine-rich peptides as a function of extracellular peptide concentration, serum, and plasma membrane associated proteoglycans, Bioconjug. Chem. 19 (2008) 656–664.
[39] J.R. Maiolo, M. Ferrer, E.A. Ottinger, Effects of cargo molecules on the cellular uptake of arginine-rich cell-penetrating peptides, Biochim. Biophys. Acta Biomembr. 1712 (2005) 161–172.
[40] G. Tünnemann, R.M. Martin, S. Haupt, C. Patsch, F. Edenhofer, M.C. Cardoso, Cargo-dependent mode of uptake and bioavailability of TAT-containing proteins and peptides in living cells, FASEB J. 20 (2006) 1775–1784.
[41] M.E. Lindgren, M.M. Hällbrink, A.M. Elmquist, U. Langel, Passage of cell-penetrating peptides across a human epithelial cell layer in vitro, Biochem. J. 377 (2004) 69–76.
[42] C. Palm, M. Jayamanne, M. Kjellander, M. Hällbrink, Peptide degradation is a critical determinant for cell-penetrating peptide uptake, Biochim. Biophys. Acta Biomembr. 1768 (2007) 1769–1776.
[43] R. Fischer, H. Hufnagel, R. Brock, A doubly labeled penetratin analogue as a ratiometric sensor for intracellular proteolytic stability, Bioconjug. Chem. 21 (2010) 64–73.
[44] M. Terasaki, K. Miyake, P.L. McNeil, Large plasma membrane disruptions are rapidly resealed by $Ca^{2+}$-dependent vesicle–vesicle fusion events, J. Cell Biol. 139 (1997) 63–74.
[45] E. Bárány-Wallje, J. Gaur, P. Lundberg, Ü. Langel, A. Gräslund, Differential membrane perturbation caused by the cell penetrating peptide Tp10 depending on attached cargo, FEBS Lett. 581 (2007) 2389–2393.
[46] L. Vasconcelos, F. Madani, P. Arukuusk, L. Pärnaste, A. Gräslund, Ü. Langel, Effects of cargo molecules on membrane perturbation caused by transportan10 based cell-penetrating peptides, Biochim. Biophys. Acta Biomembr. 1838 (2014) 3118–3129.
[47] K.W. Dunn, M.M. Kamocka, J.H. McDonald, A practical guide to evaluating colocalization in biological microscopy, Am. J. Physiol. Cell. Physiol. 300 (2011) C723–C742.